

Structural Characterization of Dissolved Organic Matter at the Chemical Formula Level using TIMS-FT-ICR MS/MS

Dennys Leyva[†], Rudolf Jaffe[†] and Francisco Fernandez Lima^{*†‡}

[†]Department of Chemistry and Biochemistry and [‡]Biomolecular Sciences Institute, Florida International University, Miami, Florida, 33199, United States

Corresponding author: *fernandf@fiu.edu.

ABSTRACT: TIMS-FT-ICR MS is an important alternative to study the isomeric diversity and elemental composition of complex mixtures. While the chemical structure of many compounds in the Dissolved Organic Matter (DOM) remains largely unknown, the high structural diversity has been described at the molecular level using chemical formulas. In this study, we further push the boundaries of TIMS-FT-ICR MS by performing chemical formula-based ion mobility and tandem MS analysis for the structural characterization of DOM. The workflow described is capable to mobility select ($R \sim 100$) and isolate molecular ion signals ($\Delta m/z = 0.036$) in the ICR cell, using single shot ejections after broadband ejections and MS/MS based on sustained off-resonance irradiation collision-induced dissociation (SORI-CID). The workflow results are compared to alternative TIMS-q-FT-ICR MS/MS experiments with quadrupole isolation at nominal mass ($\sim 1\text{Da}$). The technology is demonstrated with isomeric and isobaric mixtures (e.g., 4-Methoxy-1-naphthoic acid, 2-Methoxy-1-naphthoic acid, Decanedioic acid) and applied to the characterization of DOM. The application of this new methodology to the analysis of a DOM is illustrated by the isolation of the molecular ion $[\text{C}_{18}\text{H}_{18}\text{O}_{10}\text{-H}]^+$ in the presence of other isobars at nominal mass 393. Five IMS bands were assigned to the heterogenous ion mobility profile of $[\text{C}_{18}\text{H}_{18}\text{O}_{10}\text{-H}]^+$ and candidate structures from the PubChem database were screened based on their ion mobility and MS/MS matching score. This approach overcomes traditional challenges associated with the similarity of fragmentation patterns of DOM samples (e.g., common neutral losses of H_2O , CO_2 , and $\text{CH}_2\text{-H}_2\text{O}$) by narrowing down the isomeric candidate structures using the mobility domain.

INTRODUCTION

Critical environmental and ecological processes are strongly influenced by Dissolved Organic Matter (DOM)^{1,2}, one of the most studied natural complex mixtures. Thus, a thorough knowledge of DOM chemical composition and structure at the molecular level is essential for the understanding of its role in the aquatic environments. Although the molecular features of DOM has been the focus of a multitude of studies over the last decades²⁻⁴, the elucidation of its chemical structure and a clear view of DOM isomeric complexity, persist as one of the most challenging analytical problems.⁵⁻⁸

Analytical approaches integrating ultra-high resolution mass spectrometry, gas/liquid pre-separation techniques and tandem mass spectrometry strategies have provided much of the existing information on the chemical diversity of DOM.^{4,9-16} An online HPLC-Orbitrap MS/MS method developed by Hawkes et.al⁵, was used in an attempt to isolate single compounds in DOM samples from different ecosystems. Although the ubiquitous nature of DOM isomeric complexity was demonstrated, the proposed

procedure was unable to separate individual compounds and differentiate fragmentation patterns from specific isomers of the same chemical formula. This limitation, commonly perceived in similar studies, was likely due to two main aspects: i) LC traditional approaches are not resolutive enough to separate closely structurally related isomers, regardless of the type of chromatographic column¹², and ii) typical MS/MS experiments do not separate precursor ions within nominal mass leading to ambiguous structural interpretation, even in cases where isobaric interferences are mass resolved and fragments can be assigned with high mass accuracy.^{17,18}

Novel workflows that combine both LC and ion mobility spectrometry (IMS) have been explored to assess the DOM complexity at the level of single isomer.¹⁹⁻²¹ Lu et.al²⁰ described the integration of LC-IMS-TOF MS for the analysis of riverine DOM; while the approach allowed molecular components to be separated in both LC and IMS domains, several isomeric species shared close values of retention time and CCS, thus underestimating the isomeric coverage. In addition, the multi-precursor isolation/fragmentation at nominal mass limited the

veracity of the molecular structure assignment based on MS/MS data.

Witt et.al¹⁸ reported a negative ion mode Electrospray Ionization Fourier Transform Ion Cyclotron Resonance tandem Mass Spectrometry (ESI-FT-ICR MS/MS) method for the analysis of DOM at the chemical formula level. Sustained off-resonance irradiation collision-induced dissociation (SORI-CID) of single molecular ions mass peaks, previously isolated by Correlated Harmonic Excitation Field (CHEF) and correlated shots of isobars in the ICR cell, permitted the identification of fragmentation pathways at the chemical formula level. Despite the several advantages of this method, the high structural diversity at the isomeric level of DOM limited the candidate structural assignment.

With the advent of high-resolution ion mobility analyzers ($R > 80$), several groups have work on their integration to ultra-high resolution mass analyzers.²²⁻³¹ Our team has pioneered the integration of trapped IMS (TIMS) with FT-ICR MS since 2015 for the characterization of isomeric species in complex mixtures³². Since them, several reports have shown the unique advantages of TIMS-FT-ICR MS for the characterization of the isomeric content in complex mixtures (e.g., endocrine disruptors, glycans, water accommodated fractions of crude oils, DOM, etc.).³³⁻³⁸ While TIMS coupling to TOF-MS and FT-ICR MS showed similar performance and high reproducibility during the analysis of DOM (i.e., both MS platforms were able to capture the major trends and characteristics), as the chemical complexity at the level of nominal mass increases with m/z ($m/z > 300-350$), only the TIMS-FT-ICR MS was able to report the lower abundance compositional trends.²¹ Recently, a workflow based on TIMS-q-FT-ICR MS/MS at the level of nominal mass (i.e., 1 Da isolation) allowed for further estimation of DOM isomeric content based on ion mobility selected fragmentation patterns and core fragments.⁷ Aside from a novel estimation of the number of isomers based on MS/MS and ion mobility data, the high similarity of neutral losses in DOM MS/MS at nominal mass suggested that better isolation strategies prior to MS/MS were necessary.

In this study, we further push the boundaries of TIMS-FT-ICR MS by performing chemical formula-based ion mobility and tandem MS analysis for the structural characterization of DOM. The workflow described is capable to mobility select ($R \sim 100$) and isolate molecular ion signals ($< 36 \text{ mDa}$) in the ICR cell, using single shot ejections after broadband ejections and MS/MS based on sustained off-resonance irradiation collision-induced dissociation (SORI-CID). Taking advantage of the high ion mobility resolution ($R \sim 100$) and mass resolution ($R \sim 400,000$), chemical formula-based ion mobility and tandem mass spectrometry profiles were generated. The technology is shown for the case of an isomeric and isobaric standard mixture and a DOM standard.

EXPERIMENTAL

Sample preparation

Two isomeric standards (4-Methoxy-1-naphthoic acid and 2-Methoxy-1-naphthoic acid) and an isobaric compound at nominal mass 201 Da (Decanedioic acid) were purchased from Sigma-Aldrich (St Louis, MO) and Thermo Fisher Scientific (Ward Hill, MA) respectively. Surface water was collected from Pantanal (PAN) National Park – SE Brazil, one of the most important and biodiverse freshwater wetlands around the world. Details on sampling and sample treatment procedure can be found in this reference.² The DOM extracted sample was dissolved in Denatured Ethanol to a final concentration of 1 ppm. Prior to ESI-TIMS-FT ICR MS analysis, both the sample and standards were spiked with 5% (v/v) of low-concentration Tuning Mix (G1969-85000) from Agilent Technologies (Santa Clara, CA). All solvents used were of Optima LC-MS grade or better, obtained from Fisher Scientific (Pittsburgh, PA).

ESI Source

An Electrospray Ionization source (Apollo II ESI design, Bruker Daltonics, Inc., MA) was utilized in negative ion mode. Sample solutions were introduced into the nebulizer at 150 $\mu\text{L}/\text{h}$ using a syringe pump. Typical operating conditions were 3300-3600 V capillary voltage, 4 L/min dry gas flow rate, 1.0 bar nebulizer gas pressure, and a dry gas temperature 180 °C.

TIMS-FT-ICR MS/MS experiments

A custom built TIMS-FT-ICR MS Solarix 7T spectrometer equipped with an infinity ICR cell (Bruker Daltonics Inc., MA) was used for all the experiments. The principle on TIMS separation when coupled to the FT-ICR MS can be found in several publications of our group.^{21,38,39} Briefly TIMS relies on the utilization of an electric field to hold ions stationary against a moving gas, so that the drag force is balanced with the electric field and ions are spatially separated across the TIMS analyzer axis based on their ion mobility.⁴⁰⁻⁴² During ion mobility separation, a quadrupolar field confines the ions in the radial direction to increase trapping efficiency. The ion mobility, K , of an ion in a TIMS cell is described by the equation (1):

$$K_0 = \frac{v_g}{E} = \frac{A}{V_{\text{elution}} - V_{\text{out}}} \quad (1)$$

where v_g , E , A , V_{elution} , and V_{out} are the velocity of the gas, applied electric field, a calibration constant, elution voltage, and tunnel out voltage, respectively.

Values of K_0 can be correlated with the ion-neutral Collision Cross Section (CCS, Ω , \AA^2) using the Mason-Schamp equation (2):

$$\Omega = \frac{(18\pi)^{1/2} z}{16(k_B T)^{1/2}} \left(\frac{1}{m_i} + \frac{1}{m_b} \right)^{1/2} \frac{1760 T}{K_0 P 273.15 N^*} \quad (2)$$

where z is the charge of the ion, k_B is the Boltzmann constant, N^* is the number density, and m_i and m_b refer to the masses of the ion and bath gas, respectively.⁴³

The TIMS analyzer was controlled using an in-house software, written in National Instruments LabVIEW, and synchronized with the FTMS control acquisition program. TIMS separation was performed in the Oversampling Mode³³ using nitrogen as a bath gas at ca 300 K, $P_1 = 2.6$ and $P_2 = 0.8$ mbar, and a constant RF (2200 kHz and 140–160 Vpp). The TIMS cell was operated using a fill/trap/elute/quench sequence of 9/3/9/3 ms, a maximum of 500 IMS scans per mass spectrum and a voltage difference across the ΔE gradient of 0.05 V ($R \sim 100$). The ramp voltage gradient was stepped by 0.1 V/frame with a ΔV_{ramp} of 30 to 100 V. The deflector (V_{def}), funnel entrance (V_{fun}) and funnel out (V_{out}) voltages were $V_{\text{def}} = -120/50$ V, $V_{\text{fun}} = -70$ V and $V_{\text{out}} = -6$ V/30 V. For the case of the DOM sample, the TIMS cell was operated in a multiple accumulation mode, with an average of 20 FT scans per IMS frame (ramp voltage gradient stepped by 0.0125 V/frame) resulting in a stepped E gradient of 0.25 V/frame. A maximum of 400 IMS scans per mass spectrum was collected and a 5 V voltage difference across the ΔE gradient was established. The remaining voltage settings were kept constant.

CHEF-SORI-CID and Q-CID experiments

The precursor ions at nominal mass were pre-isolated in the quadrupole to increase the number of ions of interest in the collision cell (~ 10 m/z window), then transferred to the ICR cell and isolated with a 1 m/z notch applying Correlated Harmonic Excitation Field (CHEF)^{18,44,45} with typical 8–10 % isolation power. Each single precursor ion was preserved for further SORI activation and the remaining isobaric peaks were ejected out of the ICR cell by single shots. Argon was pulsed into the ICR cell (10 mbar pressure) and a pump delay of 3 s was used to reestablish high vacuum conditions before mass analysis. The ions were then sweep excited and finally detected with 2 MW transient. A SORI power ranged from 0.5–1% with a pulse length of 0.1–0.2 s and a frequency offset of -500 Hz were set up for SORI-CID experiments. For comparison purposes, nominal mass q-CID isolation tandem MS experiments were performed using 15–20 eV CID energies prior to injection to the FT-ICR MS.

Data processing

The TIMS-FT-ICR MS spectra were externally calibrated for ion mobility using the Agilent Tuning Mix calibration standard and the reported nitrogen mobility (K_n) values by Stow et. al.^{46,47} The MS/MS spectra were internally calibrated using the exact masses of known neutral losses in DOM.³³ The assignment of chemical formula was conducted using Data Analysis (Bruker Daltonics v 5.2) based on formula constraints of $C_xH_yO_{0-19}$, and odd and even electron configurations were allowed. TIMS spectra for each molecular formula was processed using the custom-built Software Assisted Molecular Elucidation (SAME) package – a specifically designed TIMS-MS data processing script written in Python v3.7.3. SAME package utilizes noise removal, mean gap filling, “asymmetric least

squares smoothing” base line correction, peak detection by continuous wavelet transform (CWT)-based peak detection algorithm (SciPy package), and Gaussian fitting with non-linear least squares functions (Levenberg–Marquardt algorithm).³⁹ Data was processed using Data Analysis (v. 5.2, Bruker Daltonics, CA) and all other plots were created using OriginPro 2016 (Originlab Co., MA). Candidate structures were obtained by in-silico fragmentation using the MetFrag CL tool and the PubChem database^{48,49} and theoretical CCS using the trajectory method (TM) in IMoS software version 1.09c for nitrogen as a bath gas at ca. 300 K.^{50,51}

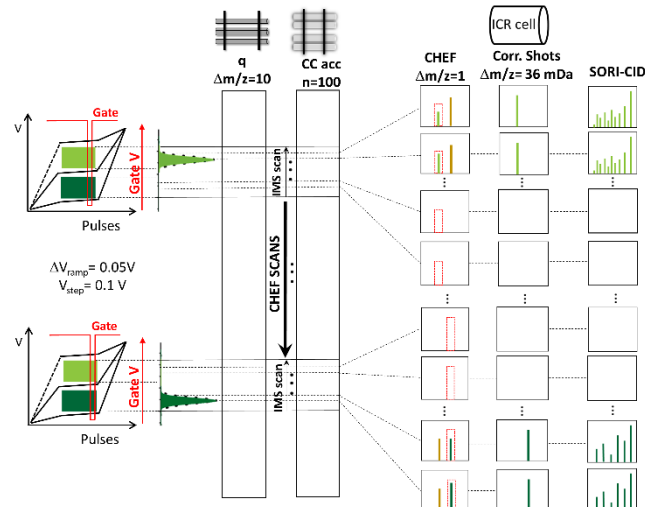


Figure 1. TIMS-q-CHEF-SORI CID MS/MS schematics. Ion mobility ranges are isolated with a 10 m/z window in the quadrupole and accumulated in the collision cell. Ions within the same mobility range injected in the ICR cell, followed by CHEF-correlated shots isolation at 0.036 m/z and SORI-CID fragmentation. After a full ion mobility scan at a single target precursor (0.036 m/z window), the next full ion mobility scan at the next precursor is generated. Example is shown for isobars with different ion mobility values (light and dark green signals).

RESULTS AND DISCUSSION

The experimental sequence for TIMS in tandem with CHEF-shots isolation and SORI CID is shown in Figure 1. Briefly, ions within a mobility range are scanned in the TIMS cell using a non-linear scan function, then pre-filtered in the quadrupole with 10 Da window and stored in the collision cell prior to the injection in the ICR cell for CHEFT+SHOTS and SORI-CID.

The target precursor is isolated in the ICR cell with a 0.036 m/z window by first applying a characteristic CHEF wave function to broadband eject ions out with a 1 m/z notch and by further ejecting isobars using correlated shots to 0.036 m/z window. Ions are fragmented using SORI-CID and a final mass spectrum is generated at ultra-high resolution ($R \sim 150,000$ –400,000). The coupling of the TIMS cell to the FT- ICR in this setting is particularly

advantageous since ions can be identified by their mobility and chemical formula. The mobility selected high-resolution isolation and fragmentation of precursor ions can provide unambiguous structural information at the level of chemical formula. This capability is very challenging, if not impossible, to achieve by traditional q-based MS/MS workflows on complex mixtures.

The capabilities of the proposed TIMS-q-CHEF-SORI CID MS/MS method is illustrated for the case of a mixture containing two isomeric standards (4-Methoxy-1-naphthoic acid and 2-Methoxy-1-naphthoic acid) and one isobaric standard (Decanedioic acid). Typical TIMS-q-CID MS/MS and TIMS-q-CHEF-SORI CID MS/MS spectra of the individual isomeric and isobaric standards are shown in Figure 2. Notice that the isobaric standard (C) cannot be separated by ion mobility from one of the isomeric standards (B and C).

The 10 m/z isolation window profiles show monoisotopic mass peaks at nominal mass 201 for $[M-H]^-$ species (A/B: $[C_{12}H_{10}O_3-H]^-$ and C: $[C_{10}H_8O_4-H]^-$). The ion mobility projections depict single IMS bands for each standard with closely related CCS values in the range of 155-160 \AA^2 . Although baseline separation of the isomeric species A and B can be achieved in the IMS domain, the isobaric compound C shares the same ion mobility as standard B. The MS/MS spectra of the standards obtained by q-CID or SORI-CID show very similar fragmentation patterns. The

MS/MS are both characterized by typical neutral losses of $-H_2O$, CO , CH_2O , and CO_2 . A closer view of the MS/MS profiles indicates that the generation of some characteristic fragments is favored when SORI-CID is used. For example, a CO_2 neutral loss generates a common fragment (m/z 157.0657) for the isomeric standards A and B either by CID or SORI-CID. However, unique fragments were found for standard A (m/z 142.0425) and B (m/z 127.0552) when in-cell fragmentation (SORI-CID) was utilized. That is, the CHEF-SORI-CID approach can be useful to identify structural isomers with distinctive fragmentation profiles. For the case of the isobar (C), apart from a water loss (m/z 183.1027) in q-CID, no clear difference in the MS/MS spectra from both fragmentation approaches was observed.

The effectiveness of the TIMS-q-CHEF-SORI CID MS/MS method to unambiguously identify each compound was assessed through the study of the isomeric and isobaric standard mixture (Figure 3). The 10 Da and nominal mass isolations of the mixture (A+B+C) resulted in two mass peaks in the MS domain corresponding to the precursor species $[A/B-H]^-$ and $[C-H]^-$ when both strategies (Q vs CHEF) were implemented (first column, Figure 3).

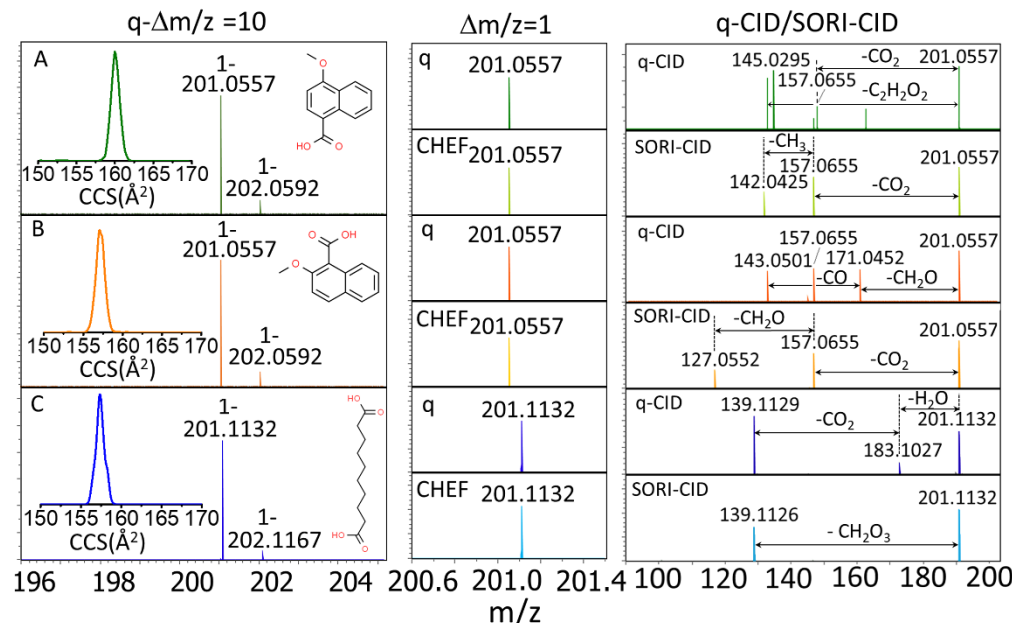


Figure 2. Comparison of ESI(-)-TIMS-q-CID MS/MS and ESI(-)-TIMS-q-CHEF-SORI CID MS/MS of individual isomeric and isobaric standards: 4-Methoxy-1-naphthoic acid (A), 2-Methoxy-1-naphthoic acid (B) and Decanedioic acid(C).

A further application of Correlated Shots permitted a single isolation ($\Delta m/z$ of 0.036) of both A/B and C in different runs by ejecting C and A/B out of the ICR cell respectively (Column 2, Figure 3). From the MS/MS spectra (Top column 3, Figure 3) and the IMS projections the standard A (green) can be unambiguously identified based

on both ion mobility and fragmentation fingerprint when the q-CID approach is used. That is, standards B and C signals overlap in both MS/MS and IMS domains, which could lead to the misassignment of the fragments, consequently biasing any further structural interpretation. Conversely, the isomeric standards A and B are identified

by both IMS and MS/MS (see characteristic fragments m/z 142.042 and m/z 127.0554) after in-cell isolation/fragmentation of the ion m/z 201.0557 in the ICR. Similarly, the standard C is singly isolated by CHEF and shots ejection of A+B and the correlation of the ion mobility projection (blue profile) with the fragmentation spectrum permitted the unambiguous identification of standard C (bottom column 3, Figure 3). The above results clearly represent a proof of concept for the structural analysis of an isobaric and isomeric complex mixture, at the level of chemical formula, combining high-resolution mobility separations with single precursor ion MS/MS in the ICR cell.

Previous analysis of DOM using non-targeted ESI-TIMS-FT-ICR MS illustrated the typical complexity observed in these samples with several thousands of m/z signals with a \pm 2 Da space regularity, as the one depicted in the isolation profile shown in the bottom of Figure 4, and around 3000 assigned chemical formulae based on accurate mass measurements⁷⁻²¹. The integration of the gas-phase separation by TIMS into the FT-ICR MS workflow and the use of a methodology based on the computation of

core fragments, neutral losses and fragmentation patterns from nominal mass CID experiments, also revealed a new complexity of DOM in the isomeric dimension. As previously discussed, the nominal mass isolation and CID fragmentation of a DOM sample could lead to an erroneous structural identification due to a false positive assignment of core and intermediate fragments arising from multiple precursors.

The TIMS-q-CHEF-SORI CID MS/MS method was applied to the structural analysis of the Pantanal DOM sample at the level of a chemical formula. The analysis of the Pantanal DOM sample combining TIMS with quadrupole isolation at nominal mass 393 Da and CID fragmentation resulted in five MS/MS profiles that share similar fragmentation patterns with typical neutral losses of H_2O , CO , CO_2 , and CH_4 (Figure 4, top row). The analysis of the ion mobility domain revealed a heterogeneous profile (CCS range 170-200 \AA^2) that can be better described with five IMS bands (See the color profile in Figure 4). Notice that additional isomers/conformers could share the same IMS band; that is, the five assigned IMS bands may contain more than five isomeric species (more details below).

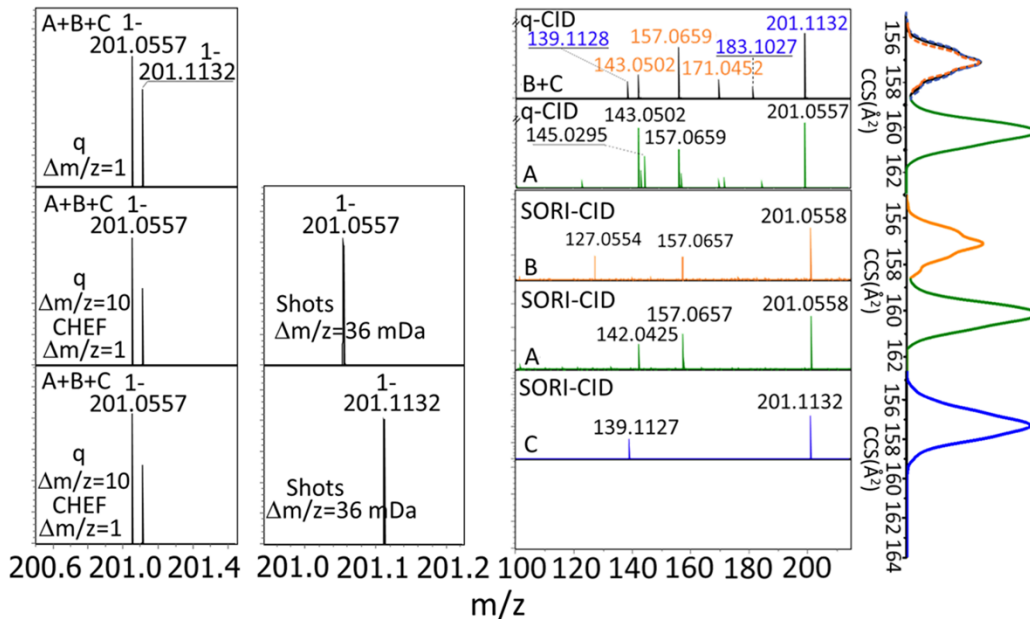


Figure 3. Comparison of TIMS-q-CID MS/MS ($\Delta m/z=1$) and TIMS-q-CHEF-SORI CID MS/MS ($\Delta m/z=0.036$) for an isobaric and isomeric standards mixture (4-Methoxy-1-naphthoic acid A, 2-Methoxy-1-naphthoic acid, B, and Decanedioic acid, C). IMS projections shown in the right corner are correlated with each corresponding MS/MS profile. Notice the overlap of both ion mobility profiles and fragment spectra of B and C when ion mobility is combined with q-CID at nominal mass (orange and blue).

Inspection of the fragmentation data generated per each IMS band using TIMS-q-CID MS/MS (See Table S1) confirmed the cooccurrence of multiple intermediate fragments (e.g. isobaric fragments at m/z 349 resulting from CO_2 losses of four different precursor ions) regardless of the IMS band analyzed. This result, once again, evidences the necessity of a clean isolation of single

precursor ions for a better structural analysis of DOM. The CHEF broadband ejection applied to a 1 Da notch at nominal mass 393 in the Pantanal DOM sample showed several m/z signals corresponding to typical $[\text{M}-\text{H}]^+$ highly oxygenated species (Figure 4, bottom). A further application of correlated shots ejections of the interferent isobars permitted a clean isolation of the $[\text{C}_{18}\text{H}_{18}\text{O}_{10}-\text{H}]^+$

precursor ion ($\Delta m/z = 0.036$). Inspection of the ion mobility domain depicted an heterogenous profile with five bands annotated using the SAME code. The collected FT-ICR MS/MS scans associated with each IMS band of the isolated ion were averaged out resulting in five fragment spectra. Dissection of the MS/MS spectra showed common fragments for all IMS bands associated with neutral losses of H_2O and CH_3OH , multiple decarboxylations ($n\text{CO}_2$ losses), and combinations among them (Table S2), in good agreement with previous observations from Witt et.al¹⁸. Moreover, characteristic fragments correlated with the IMS bands; this suggest that structural isomeric species could be identified by their ion mobility and fragmentation patterns.

Common fragments of the $[\text{C}_{18}\text{H}_{18}\text{O}_{10}-\text{H}]^-$ precursor ion found across the IMS bands were filtered out from the MS/MS data and search over PubChem database and in-silico fragmentation using Metfrag CL. Fifty candidate structures were retrieved solely based on the accurate mass of the precursor ion. Further analysis of each fragmentation data associated to the five experimental IMS bands, generated a list of 34 possible structures sorted by a score that reflects the best MS/MS match. The refined and sorted list of candidate structures per ion mobility and MS/MS scoring permitted the experimental assignments. Inspection of the heatmap in Figure 5 (top) revealed the highest Metfrag scores for the structures associated to the IMS bands 1, 3 and 5. However, the more confident assignments, based on the difference between the highest

and the second-to-highest scores among IMS bands, were found for the structures with ID 14 and 16 (IMS₃), 10 and 12 (IMS₂), 6 and 7 (IMS₁), and 26 and 27 (IMS₄). A distribution of the potential structures per IMS band constrained by the Metfrag score is shown in Figure 5 (bottom). In general, as mentioned above, the IMS₁ and IMS₃ bands group the majority of the assigned structures. While this number of potential isomeric species associated with a single chemical formula may appear high, it provides a short list considering the DOM complexity for secondary confirmation using individual standards

CONCLUSIONS

A novel TIMS-FT-ICR MS/MS workflow for the structural analysis of complex DOM samples at the level of chemical formula was developed. The integration of high-resolution ion mobility with single precursor ion isolation in the ICR with a m/z 0.036 isolation window and fragment assignment with both high resolution and mass accuracy, resulted in a versatile approach that permits the identification and structural assignment of single species from a complex mixture (i.e., mixtures containing isomeric interferences).

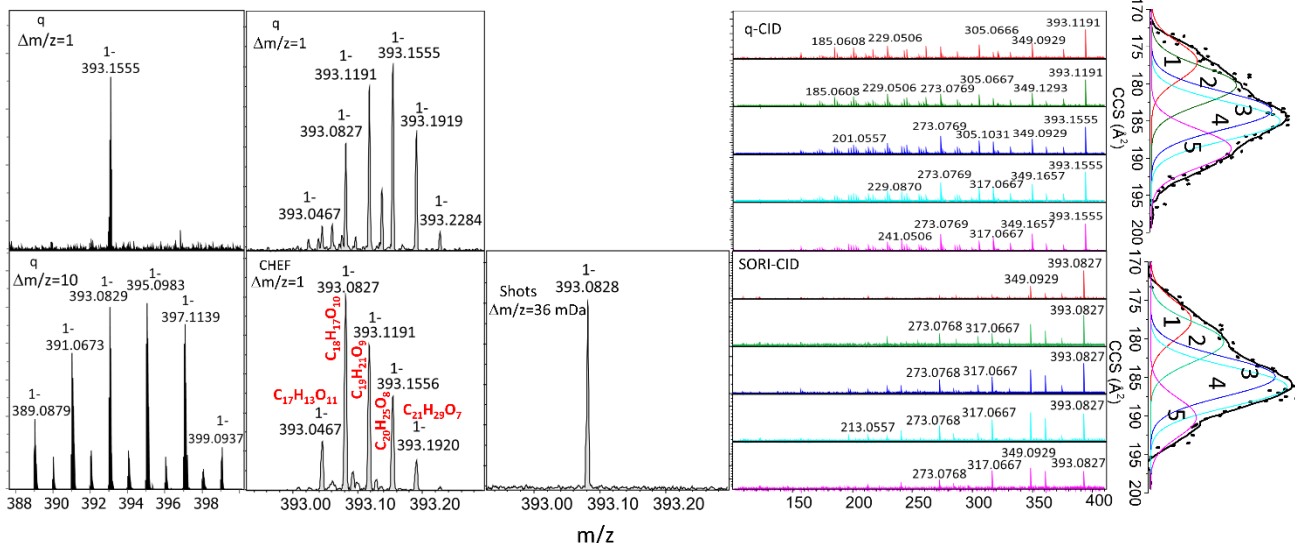


Figure 4. Comparison of TIMS-q-CID MS/MS ($\Delta m/z = 1$) and TIMS-q-CHEF-SORI CID MS/MS ($\Delta m/z = 0.036$) of the Pantanal DOM at nominal mass 393 (top row). The molecular ion $[\text{C}_{18}\text{H}_{18}\text{O}_{10}-\text{H}]^-$ isolation and SORI-CID is shown as a function of the ion mobility scans (bottom row). Ion mobility projections of the precursor ions with color annotated IMS bands are shown on the right (black dots represent the experimental data and black solid lines the best smooth fit from the SAME algorithm)

The analysis of a model mixture containing 4-Methoxy-1-naphthoic acid, 2-Methoxy-1-naphthoic acid, and Decanedioic acid (isomers and isobars, respectively) demonstrated that each single compound can be unambiguously identified, either by ion mobility or their

characteristic fragmentation spectra, thus representing a powerful approach compared to traditional nominal mass MS/MS schemes (co-isolation and fragmentation of several precursors).

The characterization of a chemical formula from a DOM sample at the nominal mass m/z 393 using the developed

procedure evidenced that a single mass peak (m/z 393.0828) can be effectively isolated from several isobaric species in the ICR cell. In the ion mobility domain, five IMS bands were assigned to the heterogenous profile of the precursor ion $[C_{18}H_{18}O_{10}-H]^-$ and correlated to the fragmentation data obtained by CHEF+SHOTS-SORI-CID MS/MS. Candidate structures from the PubChem database were screened based on their ion mobility and MS/MS matching score.

This study provides a proof of concept for the structural analysis of complex mixtures, at the level of chemical formula, combining high-resolution ion mobility separations with single precursor ion MS/MS in the ICR cell, without prior chromatographic separations.

ASSOCIATED CONTENT

Supporting Information

Tables S₁, S₂ contain the fragmentation data of the precursor ion $[C_{18}H_{18}O_{10}-H]^-$ from Pantanal sample using both the ESI-TIMS-q-FT-ICR-MS/MS (q-CID) and the ESI-TIMS-FT-ICR MS/MS (CHEF-SORI-CID) procedures with the correlated IMS bands assigned by the SAME algorithm. Table S₃ summarizes the candidate isomeric structures retrieved from PubChem database for $C_{18}H_{18}O_{10}$ and filtered based on the ESI-TIMS-FT-ICR MS/MS (CHEF-SORI-CID) fragmentation data. Theoretical Collisional Cross Sections calculated using the software IMoS is also included

The Supporting Information is available free of charge on the ACS Publications website.

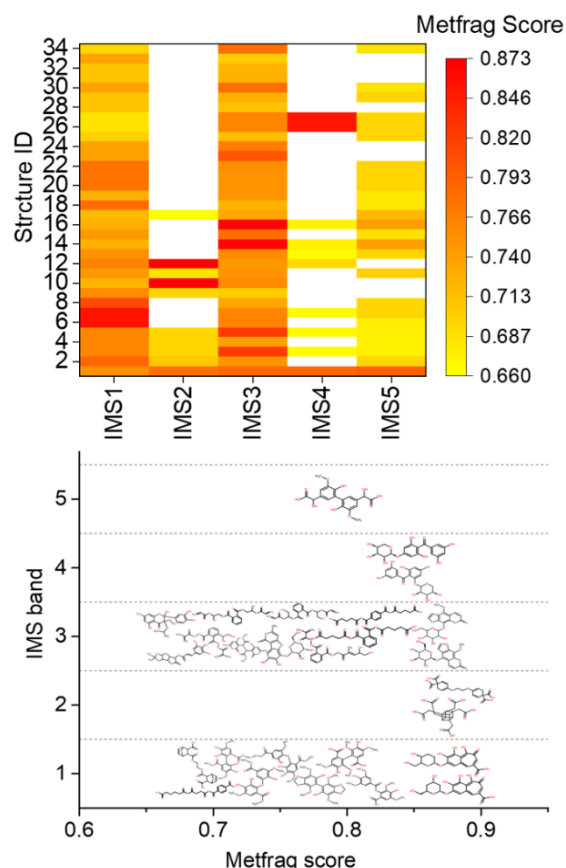


Figure 5. Candidate assignment based on ion mobility and MS/MS matching score (Metfrag CL) from PubChem database for $[C_{18}H_{18}O_{10}-H]^-$. Notice that only structures with scores higher than 0.7 were plotted. More candidate information is contained in the supporting information.

AUTHOR INFORMATION

Corresponding Author

* Ph.: 305-348-2037. Fax: 305-348-3772.
E-mail: fernandf@fiu.edu.

Author Contributions

The manuscript was written through contributions of all authors. All authors have given approval to the final version of the manuscript.

Notes

The authors declare no competing financial interest.

ACKNOWLEDGMENT

This work was supported by the National Science Foundation Division of Chemistry, under CAREER award CHE-1654274, with co-funding from the Division of Molecular and Cellular Biosciences to FFL. DL acknowledges the fellowship provided by the National Science Foundation award (HRD-1547798) to Florida International University as part of the Centers for Research Excellence in Science and Technology (CREST) Program. This is contribution number xxx from the Southeast Environmental Research Center in the Institute of Water &

Environment at Florida International University and a contribution from the Florida Coastal Everglades LTER. The authors would like to acknowledge for their technical support to the personnel of the Advance Mass Spectrometry Facility at Florida International University, and Dr. Christopher Thompson, Dr Mark E. Ridgeway and Dr. Melvin A. Park from Bruker Daltonics. RJ acknowledges the George Barley Endowment and the NSF (FCE-LTER) for partial support of this research.

REFERENCES

- Minor, E. C.; Swenson, M. M.; Mattson, B. M.; Oyler, A. R. Structural characterization of dissolved organic matter: a review of current techniques for isolation and analysis. *Environ. Sci.: Processes Impacts* **2014**, *16* (9), 2064-2079.
- Hertkorn, N.; Harir, M.; Cawley, K. M.; Schmitt-Kopplin, P.; Jaffé, R. Molecular characterization of dissolved organic matter from subtropical wetlands: a comparative study through the analysis of optical properties, NMR and FTICR/MS. *Biogeosciences* **2016**, *13* (8), 2257-2277.
- Dittmar, T. Chapter 7 - Reasons Behind the Long-Term Stability of Dissolved Organic Matter. In *Biogeochemistry of Marine Dissolved Organic Matter (Second Edition)*, Hansell, D. A.; Carlson, C. A., Eds.; Academic Press: Boston, 2015; pp 369-388.
- Lu, K.; Liu, Z. Molecular Level Analysis Reveals Changes in Chemical Composition of Dissolved Organic Matter From South Texas Rivers After High Flow Events. *Front. Mar. Sci.* **2019**, *6* (673).
- Hawkes, J. A.; Patriarca, C.; Sjöberg, P. J. R.; Tranvik, L. J.; Bergquist, J. Extreme isomeric complexity of dissolved organic matter found across aquatic environments. *Limnol. Oceanogr. Lett.* **2018**, *3* (2), 21-30.
- Zark, M.; Christoffers, J.; Dittmar, T. Molecular properties of deep-sea dissolved organic matter are predictable by the central limit theorem: Evidence from tandem FT-ICR-MS. *Mar. Chem.* **2017**, *191*, 9-15.
- Leyva, D.; Tose, L. V.; Porter, J.; Wolff, J.; Jaffé, R.; Fernandez-Lima, F. Understanding the structural complexity of dissolved organic matter: isomeric diversity. *Faraday Discuss.* **2019**, *218* (0), 431-440.
- Petras, D.; Koester, I.; Da Silva, R.; Stephens, B. M.; Haas, A. F.; Nelson, C. E.; Kelly, L. W.; Aluwihare, L. I.; Dorrestein, P. C. High-Resolution Liquid Chromatography Tandem Mass Spectrometry Enables Large Scale Molecular Characterization of Dissolved Organic Matter. *Front. Mar. Sci.* **2017**, *4* (405).
- Palacio Lozano, D. C.; Gavard, R.; Arenas-Diaz, J. P.; Thomas, M. J.; Stranz, D. D.; Mejía-Ospino, E.; Guzman, A.; Spencer, S. E. F.; Rossell, D.; Barrow, M. P. Pushing the analytical limits: new insights into complex mixtures using mass spectra segments of constant ultrahigh resolving power. *Chem. Sci.* **2019**, *10* (29), 6966-6978.
- Smith, D. F.; Podgorski, D. C.; Rodgers, R. P.; Blakney, G. T.; Hendrickson, C. L. 21 Tesla FT-ICR Mass Spectrometer for Ultrahigh-Resolution Analysis of Complex Organic Mixtures. *Anal. Chem.* **2018**, *90* (3), 2041-2047.
- Pan, Q.; Zhuo, X.; He, C.; Zhang, Y.; Shi, Q. Validation and Evaluation of High-Resolution Orbitrap Mass Spectrometry on Molecular Characterization of Dissolved Organic Matter. *ACS Omega* **2020**, *5* (10), 5372-5379.
- Patriarca, C.; Bergquist, J.; Sjöberg, P. J. R.; Tranvik, L.; Hawkes, J. A. Online HPLC-ESI-HRMS Method for the Analysis and Comparison of Different Dissolved Organic Matter Samples. *Environ. Sci. Technol.* **2018**, *52* (4), 2091-2099.
- Zark, M.; Dittmar, T. Universal molecular structures in natural dissolved organic matter. *Nat. Commun.* **2018**, *9* (1), 3178.
- Nebbioso, A.; Piccolo, A. Molecular characterization of dissolved organic matter (DOM): a critical review. *Anal. Bioanal. Chem.* **2013**, *405* (1), 109-124.
- Smith, D. F.; Blakney, G. T.; Beu, S. C.; Anderson, L. C.; Weisbrod, C. R.; Hendrickson, C. L. Ultrahigh Resolution Ion Isolation by Stored Waveform Inverse Fourier Transform 21 T Fourier Transform Ion Cyclotron Resonance Mass Spectrometry. *Anal. Chem.* **2020**, *92* (4), 3213-3219.
- Le Maître, J.; Hubert-Roux, M.; Paupy, B.; Marceau, S.; Rüger, C. P.; Afonso, C.; Giusti, P. Structural analysis of heavy oil fractions after hydrodenitrogenation by high-resolution tandem mass spectrometry and ion mobility spectrometry. *Faraday Discuss.* **2019**, *218* (0), 417-430.
- Cortés-Francisco, N.; Caixach, J. Fragmentation studies for the structural characterization of marine dissolved organic matter. *Anal. Bioanal. Chem.* **2015**, *407* (9), 2455-2462.
- Witt, M.; Fuchser, J.; Koch, B. P. Fragmentation Studies of Fulvic Acids Using Collision Induced Dissociation Fourier Transform Ion Cyclotron Resonance Mass Spectrometry. *Anal. Chem.* **2009**, *81* (7), 2688-2694.
- Gao, Y.; Wang, W.; He, C.; Fang, Z.; Zhang, Y.; Shi, Q. Fractionation and molecular characterization of natural organic matter (NOM) by solid-phase extraction followed by FT-ICR MS and ion mobility MS. *Anal. Bioanal. Chem.* **2019**.
- Lu, K.; Gardner, W. S.; Liu, Z. Molecular Structure Characterization of Riverine and Coastal Dissolved Organic Matter with Ion Mobility Quadrupole Time-of-Flight LCMS (IM Q-TOF LCMS). *Environ. Sci. Technol.* **2018**, *52* (13), 7182-7191.
- Tose, L. V.; Benigni, P.; Leyva, D.; Sundberg, A.; Ramírez, C. E.; Ridgeway, M. E.; Park, M. A.; Romão, W.; Jaffé, R.; Fernandez-Lima, F. Coupling trapped ion mobility spectrometry to mass spectrometry: trapped ion mobility spectrometry-time-of-flight mass spectrometry versus trapped ion mobility spectrometry-Fourier transform ion cyclotron resonance mass spectrometry. *Rapid Commun. Mass Spectrom.* **2018**, *32* (15), 1287-1295.
- Robinson, E. W.; Williams, E. R. Multidimensional Separations of Ubiquitin Conformers in the Gas Phase: Relating Ion Cross Sections to H/D Exchange Measurements. *J. Am. Soc. Mass Spectrom.* **2005**, *16* (9), 1427-1437.
- Robinson, E. W.; Garcia, D. E.; Leib, R. D.; Williams, E. R. Enhanced Mixture Analysis of Poly(ethylene glycol) Using High-Field Asymmetric Waveform Ion Mobility Spectrometry Combined with Fourier Transform Ion Cyclotron Resonance Mass Spectrometry. *Anal. Chem.* **2006**, *78* (7), 2190-2198.
- Robinson, E. W.; Leib, R. D.; Williams, E. R. The Role of Conformation on Electron Capture Dissociation of Ubiquitin. *J. Am. Soc. Mass Spectrom.* **2006**, *17* (10), 1470-1480.
- Saba, J.; Bonneil, E.; Pomiès, C.; Eng, K.; Thibault, P. Enhanced Sensitivity in Proteomics Experiments Using FAIMS Coupled with a Hybrid Linear Ion Trap/Orbitrap Mass Spectrometer†. *J. Prot. Res.* **2009**, *8* (7), 3355-3366.
- Ruotolo, B. T.; Hyung, S.-J.; Robinson, P. M.; Giles, K.; Bateman, R. H.; Robinson, C. V. Ion Mobility-Mass Spectrometry Reveals Long-Lived, Unfolded Intermediates in the Dissociation of Protein Complexes. *Angew. Chem. Int. Ed.* **2007**, *46* (42), 8001-8004.
- Xuan, Y.; Creese, A. J.; Horner, J. A.; Cooper, H. J. High-field asymmetric waveform ion mobility spectrometry (FAIMS) coupled with high-resolution electron transfer dissociation mass spectrometry for the analysis of isobaric phosphopeptides. *Rapid Comm. Mass Spectrom.* **2009**, *23* (13), 1963-1969.
- Bridon, G.; Bonneil, E.; Muratore-Schroeder, T.; Caron-Lizotte, O.; Thibault, P. Improvement of Phosphoproteome Analyses Using FAIMS and Decision Tree Fragmentation. Application to the Insulin Signaling Pathway in *Drosophila melanogaster* S2 Cells. *J. Prot. Res.* **2011**, *11* (2), 927-940.

29. Schrader, W.; Xuan, Y.; Gaspar, A. Studying ultra-complex crude oil mixtures by using High Field Asymmetric Waveform Ion Mobility Spectrometry (FAIMS) coupled to an ESI-LTQ-Orbitrap Mass Spectrometer. *Eur. J. Mass Spectrom.* **2014**, *20* (1), 43-49.

30. Fernandez-Lima, F. A.; Becker, C.; McKenna, A. M.; Rodgers, R. P.; Marshall, A. G.; Russell, D. H. Petroleum Crude Oil Characterization by IMS-MS and FTICR MS. *Anal. Chem.* **2009**, *81* (24), 9941-9947.

31. Fasciotti, M.; Lalli, P. M.; Klitzke, C. F.; Corilo, Y. E.; Pudenz, M. A.; Pereira, R. C. L.; Bastos, W.; Daroda, R. J.; Eberlin, M. N. Petroleomics by Traveling Wave Ion Mobility-Mass Spectrometry Using CO₂ as a Drift Gas. *Energy Fuels* **2013**, *27* (12), 7277-7286.

32. Benigni, P.; Thompson, C. J.; Ridgeway, M. E.; Park, M. A.; Fernandez-Lima, F. Targeted High-Resolution Ion Mobility Separation Coupled to Ultrahigh-Resolution Mass Spectrometry of Endocrine Disruptors in Complex Mixtures. *Anal. Chem.* **2015**, *87* (8), 4321-4325.

33. Benigni, P.; Fernandez-Lima, F. Oversampling Selective Accumulation Trapped Ion Mobility Spectrometry Coupled to FT-ICR MS: Fundamentals and Applications. *Anal. Chem.* **2016**, *88* (14), 7404-7412.

34. Pu, Y.; Ridgeway, M. E.; Glaskin, R. S.; Park, M. A.; Costello, C. E.; Lin, C. Separation and Identification of Isomeric Glycans by Selected Accumulation-Trapped Ion Mobility Spectrometry-Electron Activated Dissociation Tandem Mass Spectrometry. *Anal. Chem.* **2016**, *88* (7), 3440-3443.

35. Ridgeway, M. E.; Wolff, J. J.; Silveira, J. A.; Lin, C.; Costello, C. E.; Park, M. A. Gated trapped ion mobility spectrometry coupled to fourier transform ion cyclotron resonance mass spectrometry. *Int. J. Ion Mobility Spectrom.* **2016**, *19* (2), 77-85.

36. Benigni, P.; Marin, R.; Sandoval, K.; Gardinali, P.; Fernandez-Lima, F. Chemical Analysis of Water-accommodated Fractions of Crude Oil Spills Using TIMS-FT-ICR MS. *J. Vis. Exp.* **2017**, *121*, e55352.

37. Benigni, P.; Bravo, C.; Quirke, J. M. E.; DeBord, J. D.; Mebel, A. M.; Fernandez-Lima, F. Analysis of Geologically Relevant Metal Porphyrins Using Trapped Ion Mobility Spectrometry-Mass Spectrometry and Theoretical Calculations. *Energy Fuels* **2016**, *30* (12), 10341-10347.

38. Benigni, P.; Porter, J.; Ridgeway, M. E.; Park, M. A.; Fernandez-Lima, F. Increasing Analytical Separation and Duty Cycle with Nonlinear Analytical Mobility Scan Functions in TIMS-FT-ICR MS. *Anal. Chem.* **2018**, *90* (4), 2446-2450.

39. Benigni, P.; Sandoval, K.; Thompson, C. J.; Ridgeway, M. E.; Park, M. A.; Gardinali, P.; Fernandez-Lima, F. Analysis of Photoirradiated Water Accommodated Fractions of Crude Oils Using Tandem TIMS and FT-ICR MS. *Environ. Sci. Technol.* **2017**, *51* (11), 5978-5988.

40. Fernandez-Lima, F. A.; Kaplan, D. A.; Park, M. A. Note: Integration of trapped ion mobility spectrometry with mass spectrometry. *Rev. Sci. Instrum.* **2011**, *82* (12), 126106.

41. Fernandez-Lima, F.; Kaplan, D. A.; Suetering, J.; Park, M. A. Gas-phase separation using a trapped ion mobility spectrometer. *Int. J. Ion Mobility Spectrom.* **2011**, *14* (2), 93-98.

42. Hernandez, D. R.; DeBord, J. D.; Ridgeway, M. E.; Kaplan, D. A.; Park, M. A.; Fernandez-Lima, F. Ion dynamics in a trapped ion mobility spectrometer. *Analyst* **2014**, *139* (8), 1913-1921.

43. McDaniel, E. W.; Mason, E. A. *Mobility and diffusion of ions in gases*; John Wiley and Sons, Inc: New York, 1973.

44. Heck, A. J. R.; de Koning, L. J.; Pinkse, F. A.; Nibbering, N. M. M. Mass-specific selection of ions in Fourier-transform ion cyclotron resonance mass spectrometry. Unintentional off-resonance cyclotron excitation of selected ions. *Rapid Commun. Mass Spectrom.* **1991**, *5* (9), 406-414.

45. de Koning, L. J.; Nibbering, N. M. M.; van Orden, S. L.; Laukien, F. H. Mass selection of ions in a Fourier transform ion cyclotron resonance trap using correlated harmonic excitation fields (CHEF). *Int. J. Mass Spectrom. Ion Processes* **1997**, *165*-166, 209-219.

46. Schenk, E. R.; Ridgeway, M. E.; Park, M. A.; Leng, F.; Fernandez-Lima, F. Isomerization Kinetics of AT Hook Decapeptide Solution Structures. *Anal. Chem.* **2014**, *86* (2), 1210-1214.

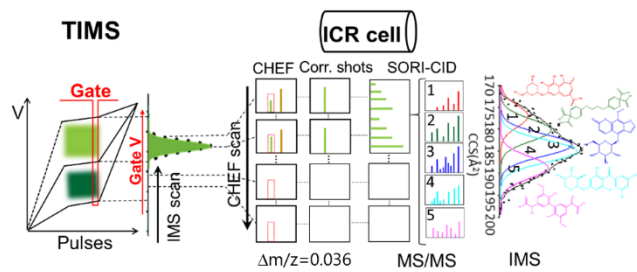
47. Stow, S. M.; Causon, T. J.; Zheng, X.; Kurulugama, R. T.; Mairinger, T.; May, J. C.; Rennie, E. E.; Baker, E. S.; Smith, R. D.; McLean, J. A.; Hann, S.; Fjeldsted, J. C. An Interlaboratory Evaluation of Drift Tube Ion Mobility-Mass Spectrometry Collision Cross Section Measurements. *Anal. Chem.* **2017**, *89* (17), 9048-9055.

48. Ruttkies, C.; Schymanski, E. L.; Wolf, S.; Hollender, J.; Neumann, S. MetFrag relaunched: incorporating strategies beyond *in silico* fragmentation. *J. Cheminf.* **2016**, *8* (1), 3.

49. Ruttkies, C.; Neumann, S.; Posch, S. Improving MetFrag with statistical learning of fragment annotations. *BMC Bioinf.* **2019**, *20* (1), 376.

50. Larriba, C.; Hogan, C. J. Ion Mobilities in Diatomic Gases: Measurement versus Prediction with Non-Specular Scattering Models. *J. Phys. Chem. A* **2013**, *117* (19), 3887-3901.

51. Larriba-Andaluz, C.; Fernández-García, J.; Ewing, M. A.; Hogan, C. J.; Clemmer, D. E. Gas molecule scattering & ion mobility measurements for organic macro-ions in He versus N₂ environments. *PCCP* **2015**, *17* (22), 15019-15029.



For Table of Contents Only